

Mingyu Li, Patrick Page-McCaw, and Wenbiao Chen



## FGF1 Mediates Overnutrition-Induced Compensatory $\beta$ -Cell Differentiation



*Diabetes* 2016;65:96–109 | DOI: 10.2337/db15-0085

**Increased insulin demand resulting from insulin resistance and/or overnutrition induces a compensatory increase in  $\beta$ -cell mass. The physiological factors responsible for the compensation have not been fully characterized. In zebrafish, overnutrition rapidly induces compensatory  $\beta$ -cell differentiation through triggering the release of a paracrine signal from persistently activated  $\beta$ -cells. We identified *Fgf1* signaling as a key component of the overnutrition-induced  $\beta$ -cell differentiation signal in a small molecule screen. *Fgf1* was confirmed as the overnutrition-induced  $\beta$ -cell differentiation signal, as inactivation of *fgf1* abolished the compensatory  $\beta$ -cell differentiation. Furthermore, expression of human *FGF1* solely in  $\beta$ -cells in *fgf1*<sup>-/-</sup> animals rescued the compensatory response, indicating that  $\beta$ -cells can be the source of FGF1. Additionally, constitutive secretion of FGF1 with an exogenous signal peptide increased  $\beta$ -cell number in the absence of overnutrition. These results demonstrate that *fgf1* is necessary and *FGF1* expression in  $\beta$ -cells is sufficient for the compensatory  $\beta$ -cell differentiation. We further show that FGF1 is secreted during prolonged activation of cultured mammalian  $\beta$ -cells and that endoplasmic reticulum stress acts upstream of FGF1 release. Thus, the recently discovered antidiabetes function of FGF1 may act partially through increasing  $\beta$ -cell differentiation.**

Like other critical physiologic factors, blood glucose levels are maintained appropriately by multiple positive and negative feedback mechanisms. Insulin from pancreatic  $\beta$ -cells is the principal glucose-lowering hormone. In conditions of insulin resistance, not only do pancreatic  $\beta$ -cells become more active but new  $\beta$ -cells are also generated to expand the capacity of insulin production through both self-replication and neogenesis or differentiation (1,2). Defects

in compensatory  $\beta$ -cell mass expansion may contribute to susceptibility to type 2 diabetes (3). Understanding its molecular mechanism should aid the prognosis of and provide new therapeutic targets for type 2 diabetes.

The molecular mechanism underlying compensatory  $\beta$ -cell genesis is not well understood, particularly for neogenesis. Evidence for both circulating factors and local signals exists. Islet transplantation and parabiosis studies have suggested a circulating factor or factors that mediate  $\beta$ -cell replication in insulin resistance (4,5), although the identity of the factor(s) remains elusive. A number of circulating factors have been shown to be able to promote  $\beta$ -cell replication, including gut hormones glucagon-like peptide-1 (GLP-1) and gastric inhibitory polypeptide (GIP); adipokines leptin and adiponectin; myokine interleukin (IL)-6; macrophage factors IL-1 $\beta$ , tumor necrosis factor (TNF)- $\alpha$ , and interferon (INF) $\gamma$ ; bone factor osteocalcin; thyroid hormones T3 and T4; liver-derived fibroblast growth factor (FGF)21; and platelet-derived growth factor (PDGF) (reviewed in Bouwens and Rooman [6], Bernal-Mizrachi et al. [7], and Kulkarni et al. [8]). The paracrine/autocrine action of insulin has been shown to be essential for insulin resistance-induced  $\beta$ -cell replication (9). Much less is known about compensatory neogenesis. Although transgenic overexpression of INF $\gamma$  in the  $\beta$ -cells (10), or transforming growth factor- $\alpha$  (TGF- $\alpha$ ) in pancreatic ductal cells (11), can induce postnatal  $\beta$ -cell differentiation, a physiological factor for compensatory  $\beta$ -cell differentiation has not been described.

FGF1, also known as acidic FGF, is a well-known growth factor. It binds to all four FGF receptors (12) and has been shown to play various roles in cell proliferation, migration, and differentiation during several biological processes, including development, angiogenesis, inflammation, and adipogenesis (reviewed in Zakrzewska et al. [13] and Raju et al. [14]). Surprisingly, however, *Fgf1*<sup>-/-</sup>

Department of Molecular Physiology and Biophysics, Vanderbilt University School of Medicine, Nashville, TN

Corresponding author: Wenbiao Chen, wenbiao.chen@vanderbilt.edu.

Received 16 January 2015 and accepted 22 September 2015.

This article contains Supplementary Data online at <http://diabetes.diabetesjournals.org/lookup/suppl/doi:10.2337/db15-0085/-/DC1>.

© 2016 by the American Diabetes Association. Readers may use this article as long as the work is properly cited, the use is educational and not for profit, and the work is not altered.

mice are viable and fertile with no overt phenotype (15), possibly due to compensation from other FGFR ligands. Recently, however, a metabolic phenotype has been discovered in *Fgf1*<sup>-/-</sup> mice (16). Further, injection of recombinant FGF1 into mice alleviates hyperglycemia in a mouse model of diabetes (17). Unlike most growth factors, FGF1 does not have a signal peptide and thus is not secreted through the vesicular system (18,19). It is exported as a multiprotein complex and Cu<sup>2+</sup> is required for the assembly of the complex and FGF1 release (18). The regulation of FGF1 secretion is poorly understood, although cell stress has been implicated. In cultured cells, several environmental stress conditions, including heat shock, hypoxia, serum starvation, and exposure to LDLs, promote FGF1 release (20–22).

We have previously developed a model of compensatory  $\beta$ -cell differentiation in zebrafish (23). Using this system, we found that the compensatory response requires prolonged excitation of existing  $\beta$ -cells, which acts non-cell autonomously to induce  $\beta$ -cell differentiation, likely by emitting a paracrine signal or signals (24). Using pharmacological and genetic analyses, here we identify FGF signaling and *Fgf1* as a mediator of overnutrition-induced  $\beta$ -cell differentiation.

## RESEARCH DESIGN AND METHODS

### Zebrafish Strains and Maintenance

Zebrafish (*Danio rerio*) were raised in an Aquatic Habitats system on a 14:10-h light-dark cycle at 28°C. Embryos were obtained from natural crossing and raised according to standard methods. Animals were staged by hours post-fertilization (hpf) and days postfertilization (dpf) (25).  $\beta$ -Cells were marked with *Tg(-1.2ins:H2BmCherry)* (23). *mnx1*-positive  $\beta$ -cells were marked with *Tg(-1.2ins:EGFP)* and *Tg(-5.1mnx1:tagRFP)* (23).

### Drug Treatment and Small Molecule Screening

For egg yolk feeding, chicken eggs were obtained from local grocery stores, and the yolk was separated and diluted to 5% by volume with 0.3 $\times$  Danieau solution as previously described (26). All drugs were made in 1,000 $\times$  stock solution and stored in light-protected Eppendorf tubes at -20°C. NBI-31772 (5 mmol/L; Sigma-Aldrich), linsitinib (10 mmol/L; LC laboratories), H-89 (10 mmol/L; LC laboratories), AICAR (100 mmol/L; LC laboratories), afatinib (10 mmol/L; LC laboratories), SB431542 (10 mmol/L; Selleckchem), DAPT (10 mmol/L; Sigma-Aldrich), SU5402 (15 mmol/L; Calbiochem and Tocris), neocuproine (10 mmol/L; Sigma-Aldrich), PD0325901 (10 mmol/L; Sigma-Aldrich), U0126 (10 mmol/L; LC laboratories), and TUDCA (0.5 mol/L; Calbiochem) were dissolved in DMSO at the indicated concentrations. NVP-AEW541 (10 mmol/L; Cayman Chemicals), vatalanib (10 mmol/L; LC Laboratories), and SAG (10 mmol/L; EMD Millipore) were dissolved in water. CyA (10 mmol/L; LC Laboratories) was dissolved in ethanol.

Induction of transgene expression of *Kir6.2*<sup>DN</sup> was performed as previously described (24). SU5402 was added after 16 h of the induction for an 8-h treatment.

### Establishment and Identification of Transgenic and Mutant Lines

New transgenic lines were generated using the Tol2 transposon system (27). The transgenes were assembled using a multisite Gateway system (28). For the FGF1 expression transgenes, *Tg(-1.2ins:FGF1)* and *Tg(-1.2ins:spFGF1)* were assembled in pDestTol2-CG2 destination vector. These transposons also carried the *cmlc2:EGFP* element, which facilitates identification of transgenic carriers (see Fig. 4C and E). *spFGF1* contains a sequence encoding a signal peptide before the *FGF1* coding sequence.

The candidate TALEN target sequences of *fgf1* were designed online using TALEN Targeter (<https://tale-nt.cac.cornell.edu/>). The target sequences are shown in Supplementary Fig. 6A and B. The repeat-variable di-residue (RVD) sequence of *fgf1* TALEN pair is NI-NG-NN-NI-NG-NN-NN-NI-NN-NN-NI-NG-NG-NG-HD-NI-HD-HD-NG (left) and NN-HD-NG-NN-HD-NG-HD-HD-NI-NN-HD-HD-NI-HD-NG-NN-NG (right). The left RVDs were assembled in pTAL3 and the right RVDs were assembled in pTAL4 vector using Golden Gate TALEN assembly kit (29). The final TALEN construct was used for mRNA synthesis using T3 mMessage mMachine Transcription Kit (Ambion, Austin, TX) according to the manufacturer's instructions. An equal amount of the mRNA for the TALEN pair was mixed and 200 pg of the mixture was microinjected into each zebrafish embryo at the one-cell stage. The efficiency of TALEN was detected by T7 Endonuclease I (New England BioLabs, Ipswich, MA) digestion. First, a 418-bp genomic DNA fragment containing the target site was amplified from genomic DNA of injected embryos using primers 5'-GCACGTTTCTGCCAGCTGCTC-3' (FGF1-TNF) and 5'-CTGCAAAGCTGTAGGTCCAAATGTTC-3' (FGF1-TNR). The PCR product was denatured and annealed in a thermocycler using a program of 95°C for 5 min, 95 to 85°C at -2°C/s, and 85 to 25°C at -0.1°C/s. The products were digested by T7 Endonuclease I at 37°C for 1 h and resolved by electrophoresis in a 1.5% agarose gel.

To identify mutation carriers, genomic DNA from the tail fin of individual F1 fish was subjected to PCR and the T7 Endonuclease I assay as described above. The T7 Endonuclease I-cleavable PCR products were sequenced to identify desirable mutations. F1s with 5-bp deletion (*mu1*) and 7-bp deletion (*mu2*) were selected. To identify *mu1* carriers, PCR products amplified using FGF1-TNF and FGF1-TNR primers as described above, then digested with BstYI, whose target site is absent in the WT allele. To identify *mu2* carriers, an allele-specific primer was used for PCR genotyping.

### Immunofluorescence and Imaging

The *fgf1*<sup>*mu1/mu1*</sup>; *Tg(-1.2ins:FGF1; CG); Tg(-1.2ins:H2BmCherry)* or *Tg(-1.2ins:spFGF1; CG); Tg(-1.2ins:H2BmCherry)* larvae were stained with anti-FGF1 antibody (1:200, ab9588; Abcam), followed by Alexa Fluor 488-conjugated secondary antibody (1:3,000) using standard techniques. All images

were collected using a Zeiss LSM710 confocal microscope (Carl Zeiss).

### Lineage Tracing

Cre-mediated lineage tracing of pancreatic Notch-responsive cells (PNCs) was performed as previously described (30,31). Progeny of *Tg(Tp1:creER<sup>T2</sup>);Tg( $\beta$ actin:loxP-stop-loxP-hmgb1-mCherry)* crossed with *Tg(-1.2ins:eGFP)* were treated with 4-hydroxytamoxifen (4OHT, T176; Sigma-Aldrich) from 24 to 48 hpf, or 56 to 80 hpf. The triple-positive fish were selected under fluorescent microscope at 4 dpf for the analysis.

Lineage tracing using retention of H2B-EGFP was performed as previously described (32,33). H2B-EGFP mRNA (100 pg) was injected into *Tg(-1.2ins:H2B-mCherry)* embryos at the one-cell stage. Anti-GFP (1:500; Abcam) and Alexa Fluor 568 antibodies (1:2,000; Life Technologies) were used to amplify the signal.

### $\beta$ -Cell Counting

Counting of  $\beta$ -cells was performed as described previously (23,24). In brief, after fixation in 4% paraformaldehyde overnight in 4°C, larvae were washed with 1 $\times$  PBS plus 0.1% Tween-20 (PBST) and flat mounted in Aqua-Mount (Richard-Allan Scientific) with their right side facing the coverslip. The larvae were slightly flattened to facilitate counting of individual nuclei. The  $\beta$ -cells were counted using the nuclear mCherry signal using a Zeiss AxioImager under a 40 $\times$  lens or using confocal projections taken by a Zeiss LSM710 under a 40 $\times$  lens (Carl Zeiss).

### Total Glucose Assay

Total glucose was determined using the Amplex Red Glucose/Glucose Oxidase Assay Kit (Life Technologies, Grand Island, NY). A pool of 10 larvae was homogenized in 100  $\mu$ L of sample buffer. The homogenate was spun at 13,000 rpm for 5 min. Free glucose in 10  $\mu$ L of supernatant (equivalent of one larva) was determined according to the manufacturer's instructions. Fluorescence (excitation, 535 nm; emission, 590 nm) was measured using a SpectraMax M5 Microplate Reader (Molecular Devices). At least five pools of each sample were measured.

### FACS and RT-PCR

Anesthetized *Tg(-1.2ins:H2BmCherry)* larvae were collected in a 1.5-mL Eppendorf tube containing collagenase P (0.6 mg/mL) plus tricaine (0.02%). They were lightly crushed and incubated in 37°C for 5 min. The lysate was spun and pellet resuspended in cold Hanks' balanced salt solution (HBSS) plus 10% FCS plus collagenase P. The suspension was transferred to a 6-cm petri dish on ice, and large clusters of somatic tissue were removed using a pair of forceps. The remaining small tissue bits (mostly gastrointestinal tissues) were transferred in a 1.5-mL Eppendorf tube. The samples were digested with Liberase DH (100  $\mu$ g/mL) at 33°C for 50 min, spun, and pellet resuspended in cold and fresh Liberase DH in HBSS plus 10% FCS. Single-cell suspensions were obtained by passing homogenates through 40- $\mu$ m mesh,

followed by 20- $\mu$ m mesh. Single-cell suspension from non-transgenic wild-type larvae was prepared in parallel as a negative control for gating. The samples were kept on ice prior to flow cytometry. The mCherry-positive  $\beta$ -cells were collected using the BD FACS Aria II in the Vanderbilt University Medical Center (VUMC) Flow Cytometry Core.

Total RNA was extracted from  $\beta$ -cells and whole larvae using Trizol Reagents (Invitrogen) and digested by the RQ1 RNase-Free DNase (Promega) to remove any genomic DNA contamination. First-strand cDNA was synthesized using Moloney Murine Leukemia Virus Reverse Transcriptase (Promega) with oligo(dT)<sub>16</sub> as first-strand primers according to the manufacturer's instructions. The PCR primers used were as follows: *fgf1*, 5'-GAAAACACA TACAGCATACTGCGCAT-3' and 5'-TCGTGGAAGAAAGA AAATGGCC-3'; *insa*, 5'-TAAGCACTAACCCAGGCACA-3' and 5'-GATTTAGGAGGAAGGAAACC-3; *gaga*, 5'-ATTTG CTGGTGTGTGTTGGA-3' and 5'-AATGCCTCTTCATGGTC GTC-3'; and *amy2a*, 5'-GGCTCCACAATCTCAACTCG-3' and 5'-CCCAGCTTGGCACCATACTTG-3'. PCR was performed using 94°C for 3 min and then 35 cycles of 30 s at 95°C, 30 s at 60°C, and 30 s at 72°C, and final extension at 72°C for 5 min.

### Cell Culture, Generation of FGF1 Lines, and Detection of Secreted FGF1

INS-1 832/13 (34) cells were provided by Dr. Christopher Newgard (Duke University) and were grown in RPMI 1640 (11.1 mmol/L glucose) supplemented with 10% FBS, 1 mmol/L sodium pyruvate, 10 mmol/L HEPES, 2 mmol/L L-glutamine, 50  $\mu$ mol/L  $\beta$ -mercaptoethanol, 100 units/mL penicillin, and 100  $\mu$ g/mL streptomycin. Cells were incubated at 37°C in a 5% CO<sub>2</sub> incubator.

The complete coding sequence of human FGF1 was subcloned into the pcDNA3.1-Puro-CAG vector, resulting in a pcDNA3.1-Puro-CAG-FGF1 vector. INS-1 832/13 cells were transfected with Lipofectamine 2000 (Life Technologies) according to the manufacturer's instructions. The transfected cells were selected under 5  $\mu$ g/mL puromycin (Life Technologies) for 1 week, and the selection media was changed every 1–2 days.

At 70–80% confluence, the cells were washed twice with PBS and then cultured in reduced serum media (2% FBS supplemented with 5 units/mL heparin; Sigma-Aldrich). Cells were treated for the indicated period with 100 nmol/L glibenclamide (Sigma-Aldrich), 5  $\mu$ mol/L neocuproine (Sigma-Aldrich), 10  $\mu$ mol/L U0126 (Sigma-Aldrich), 100  $\mu$ mol/L TUDCA (Calbiochem), and 5  $\mu$ g/mL tunicamycin (Sigma-Aldrich) as indicated. Conditioned media was collected, spun at 1,000g for 10 min, and filtered with 0.2- $\mu$ m filter. The clear media was concentrated by Amicon Ultra 2-mL 10K centrifugal filters (EMD Millipore) eightfold. FGF1 was detected by Western blot with the anti-FGF1 primary antibody (Abcam) and an IR700-conjugated secondary (Rockland). The Western membranes were scanned on an Odyssey system (LiCor) and analyzed using ImageJ software.

### Transmission Electron Microscopy and Endoplasmic Reticulum Lumen Width Measurement

Transmission electron microscopy of zebrafish  $\beta$ -cells was performed in the Cell Imaging Shared Resource core of the VUMC. Fish were anesthetized with 0.02% tricaine and fixed immediately in 4% glutaraldehyde, 1% PFA, 0.05 mol/L cacodylate, 1 mmol/L MgSO<sub>4</sub>, and 1% sucrose for 1.5 h. Thick sections (500 nm) were used to verify position for thin (~70 nm) sectioning. Images were taken using a Philips/FEI T-12 microscope.  $\beta$ -Cells were identified by the morphology. The width of the rough endoplasmic reticulum (ER) lumen for five cells in each group at 20 or more positions per cell was measured blind to the origin of the tissue.

Data are means and SEs. Data were analyzed by one-way ANOVA followed by Fisher post hoc test or Student *t* test (SPSS, Chicago, IL). Significance was accepted at  $P < 0.05$ .

## RESULTS

### Small Molecule Screening Implicates FGF Signaling in Overnutrition-Induced $\beta$ -Cell Differentiation

Larval stage zebrafish during sustained overnutrition (8 h of feeding chicken egg yolk) increase  $\beta$ -cell count by 25% (23). These new  $\beta$ -cells arise from *nkx2*-expressing or *mnx1*-expressing precursor cells in the peri- and intraslet area. We have previously demonstrated that the  $\beta$ -cell itself acts as the primary sensor of overnutrition (24). This raises the question of how  $\beta$ -cells signal to the precursor cells to drive differentiation into new  $\beta$ -cells. To identify the signaling system(s) that communicates the overnutrition signal, we took advantage of the pharmacological tractability of zebrafish and screened small molecule modulators of several signaling pathways implicated in  $\beta$ -cell development. These compounds were administered to 6-dpf larvae in nutrient-free (unfed control) embryo medium or in 5% chicken egg yolk in embryo medium (overnutrition condition) for 8 h, and the number of  $\beta$ -cells in each larva was counted. Compounds activating IGF-1 (NBI-31772), AMPK (AICAR), and Hedgehog (SAG) were found to have no effect on the number of  $\beta$ -cells either in control or overnutrition conditions. Compounds inhibiting IGF-1R (NVP-AEW541), PKA (H-89), EGFR (Afatinib), VEGFR (Vatalanib), TGF- $\beta$  (SB431542), Hedgehog (cylopamine or CyA), or Notch (DAPT) signaling also had no effect. In contrast, linstinib, SU5402, and U0126 significantly inhibited compensatory  $\beta$ -cell differentiation (Fig. 1A and B). We focused on understanding the effect of SU5402 and U0126. SU5402 inhibits all FGFRs, as well as VEGFR2 and PDGFR (35). Using other inhibitors, we excluded a role of VEGFR2 and PDGFR $\beta$  in compensatory  $\beta$ -cell differentiation (Supplementary Fig. 1), leaving FGFRs as the likely target of the inhibitory effect. U0126 is a well-known MEK inhibitor. Since a more potent MEK inhibitor, PD0325901, had no effect, U0126 likely acted independently of MEK. Interestingly, U0126 is a known

copper chelator (36), and FGF1 secretion requires copper (18). We hypothesized that U0126 acts by inhibiting Fgf1 release. To test the hypothesis that the compensatory  $\beta$ -cell differentiation is dependent on copper, we determined whether the specific copper chelator, neocuproine (37), could inhibit overnutrition-induced  $\beta$ -cell differentiation. Indeed, neocuproine (5  $\mu$ mol/L) significantly inhibited the compensatory  $\beta$ -cell differentiation, supporting our hypothesis (Fig. 1C). Thus, the data suggest that our screen identified two compounds acting on the FGF signaling pathway, with U0126 inhibiting the release of Fgf1 and SU5402 suppressing the FGFRs.

We considered the possibility that suppression of FGF signaling could reduce the number of  $\beta$ -cells by causing newly differentiated  $\beta$ -cells to die during overnutrition. However, SU5402 had no effect on  $\beta$ -cell number in unfed animals, indicating that SU5402 is not toxic to these cells in the unfed state. We also could find no evidence for apoptotic nuclei in  $\beta$ -cells either in overnutrition or unfed fish (Supplementary Fig. 2).

To further explore the origin of these new  $\beta$ -cells, we performed lineage tracing experiments. The PNCs have been shown to give rise to the postdevelopmental  $\beta$ -cells (30,31). However no increase of PNC-derived  $\beta$ -cells was found in the overnutrition group (Supplementary Fig. 3A). The dorsal bud-derived label-retaining cells (LRCs) have been shown to contribute to  $\beta$ -cell neogenesis after ablation (32,33). Our results indicated that the number of LRC-derived  $\beta$ -cells were not changed upon overnutrition, whereas the number of non-LRC-derived  $\beta$ -cells increased, suggesting that the new  $\beta$ -cells were ventral bud derived (Supplementary Fig. 3B and C). Moreover, SU5402 blocked the increase of these ventral bud-derived new  $\beta$ -cells (Supplementary Fig. 3B and C).

To determine whether suppression of FGF signaling blocks overnutrition-induced  $\beta$ -cell differentiation from the known precursor cells, we determined the effect of SU5402 on the number of  $\beta$ -cells with *mnx1* promoter activity. We have previously reported that the *mnx1* promoter is active in a subset of the precursors of the newly differentiated  $\beta$ -cells (23); if SU5402 blocks differentiation of these precursors, the number of TagRFP-positive  $\beta$ -cells in *Tg(-1.2ins:EGFP);Tg(-5.1mnx1:tagRFP)* fish should not increase during overnutrition. Indeed, in overnutrition animals treated with SU5402, the number of TagRFP-positive  $\beta$ -cells was not significantly changed compared with unfed animals, whereas vehicle-treated controls with overnutrition responded normally (Fig. 2A and B).

To confirm that SU5402 affected the same overnutrition-driven signal originating in the  $\beta$ -cells described previously (24), we assessed the effect of SU5402 on  $\beta$ -cell differentiation induced by pharmacological and genetic inhibition of KATP channels. We have previously shown that an 8-h treatment with an inhibitor of KATP channels,

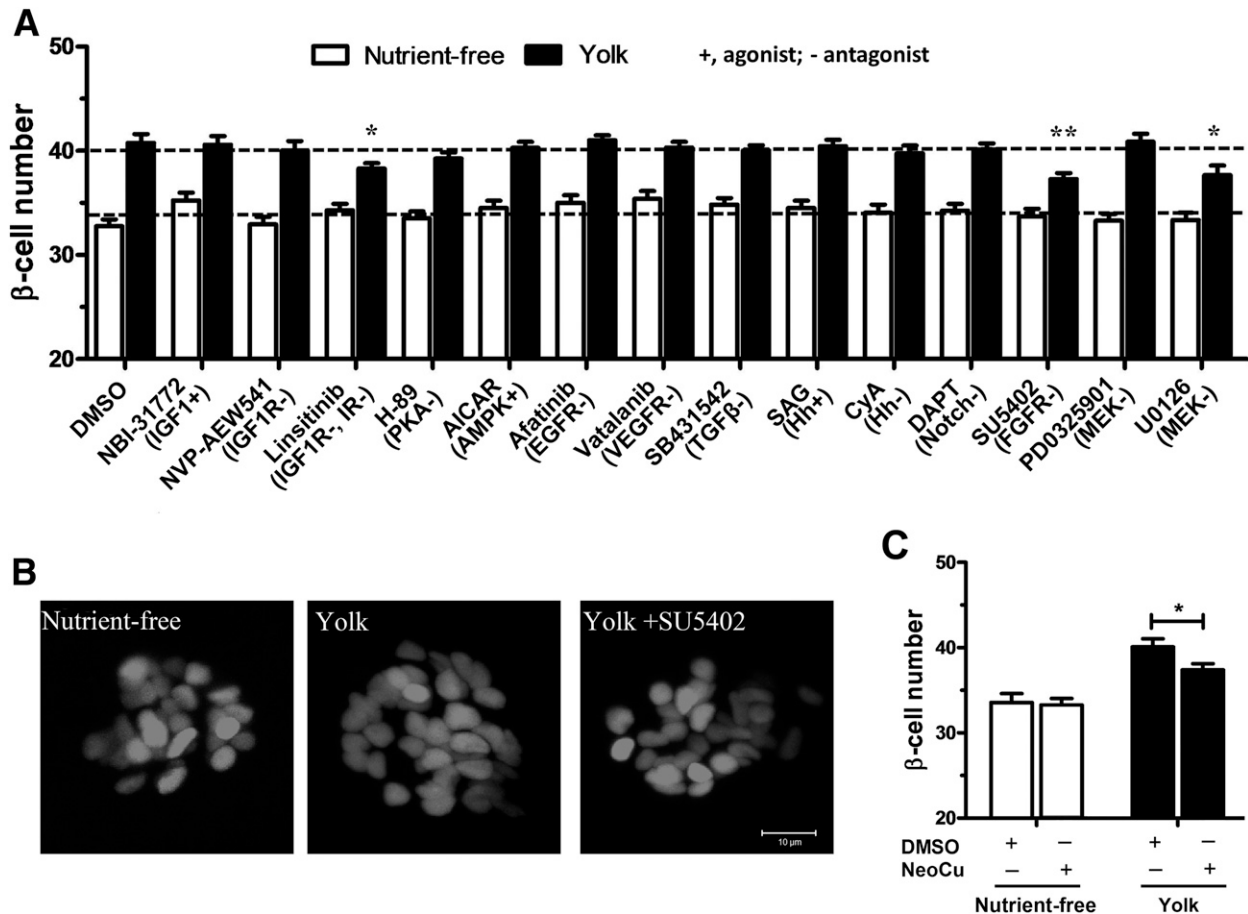


**Figure 1**—The FGF signaling pathway is involved in overnutrition-induced  $\beta$ -cell differentiation. **A**: Effects of selected small molecules on overnutrition-induced  $\beta$ -cell differentiation. 6-dpf *Tg(-1.2ins:H2B-mCherry)* larvae were cultured for 8 h in nutrient-free medium (open bars) or 5% egg yolk (filled bars) in the presence or absence of the indicated compounds. The compound name, targets, and mode of action (“+” for agonism and “-” for antagonism) are indicated on the *x*-axis. Lower dotted line is the average  $\beta$ -cell number of all larvae in nutrient-free medium, and the upper dotted line is the average  $\beta$ -cell number of all larvae in 5% yolk.  $n = 20$ –30; mean  $\pm$  SE. \* $P < 0.05$  vs. the DMSO plus yolk sample; \*\* $P < 0.01$  vs. the DMSO plus yolk sample. **B**: Representative confocal projections of  $\beta$ -cells of 6-dpf *Tg(-1.2ins:H2B-mCherry)* larvae cultured for 8 h in nutrient-free medium, 5% egg yolk, or 5% egg yolk plus SU5402. Scale bar indicates 10  $\mu$ m. **C**: Neocuproine inhibition of overnutrition-induced  $\beta$ -cell differentiation. 5-dpf *Tg(-1.2ins:H2B-mCherry)* animals were incubated in DMSO or 5  $\mu$ mol/L neocuproine overnight (16 h) to deplete  $\text{Cu}^{2+}$  before being cultured for 8 h in nutrient-free or 5% egg yolk solution containing DMSO or neocuproine.

glibenclamide, is sufficient to induce  $\beta$ -cell differentiation in zebrafish larvae in the absence of overnutrition (24). As for overnutrition, SU5402 inhibited glibenclamide-induced  $\beta$ -cell differentiation (Fig. 2C). Similarly, we had previously demonstrated that blocking KATP channel activity specifically in  $\beta$ -cells through the inducible expression of a dominant-negative KATP channel,  $\text{KIR6.2}^{\text{DN}}$ , is sufficient to induce differentiation of new  $\beta$ -cells in the absence of overnutrition (24). The same results were obtained in this study (Fig. 2D). SU5402 blocked the effect of  $\text{KIR6.2}^{\text{DN}}$  expression on  $\beta$ -cell differentiation (Fig. 2D), demonstrating that the  $\beta$ -cell-derived signal driving differentiation of  $\beta$ -cells is dependent on FGF signaling.

To further validate the role of FGF signaling in the compensatory  $\beta$ -cell differentiation, we determined whether overnutrition increases the expression of FGF target genes in the tissue surrounding and within the

islet. Following overnutrition, we observed an increase in the expression of FGF target genes, *erm* and *spry4* (38), in the islet and its surrounding tissue, which was blocked by SU5402 (Supplementary Fig. 4). These data are consistent with a model in which there is increased FGF signaling in the peri-islet tissue following overnutrition and coincident with overnutrition-induced  $\beta$ -cell differentiation.

#### Fgf1 Is Necessary for Overnutrition-Induced $\beta$ -Cell Differentiation

To test whether *Fgf1* is the ligand that initiates the signaling, we determined whether it is expressed in zebrafish  $\beta$ -cells. Zebrafish  $\beta$ -cells were isolated by FACS from 6-dpf *Tg(-1.2ins:H2B-mCherry)* larvae, and RT-PCR was performed. We found that *fgf1* mRNA is easily detectable in  $\beta$ -cells (Fig. 3A). In addition to *fgf1*, *fgf2* and

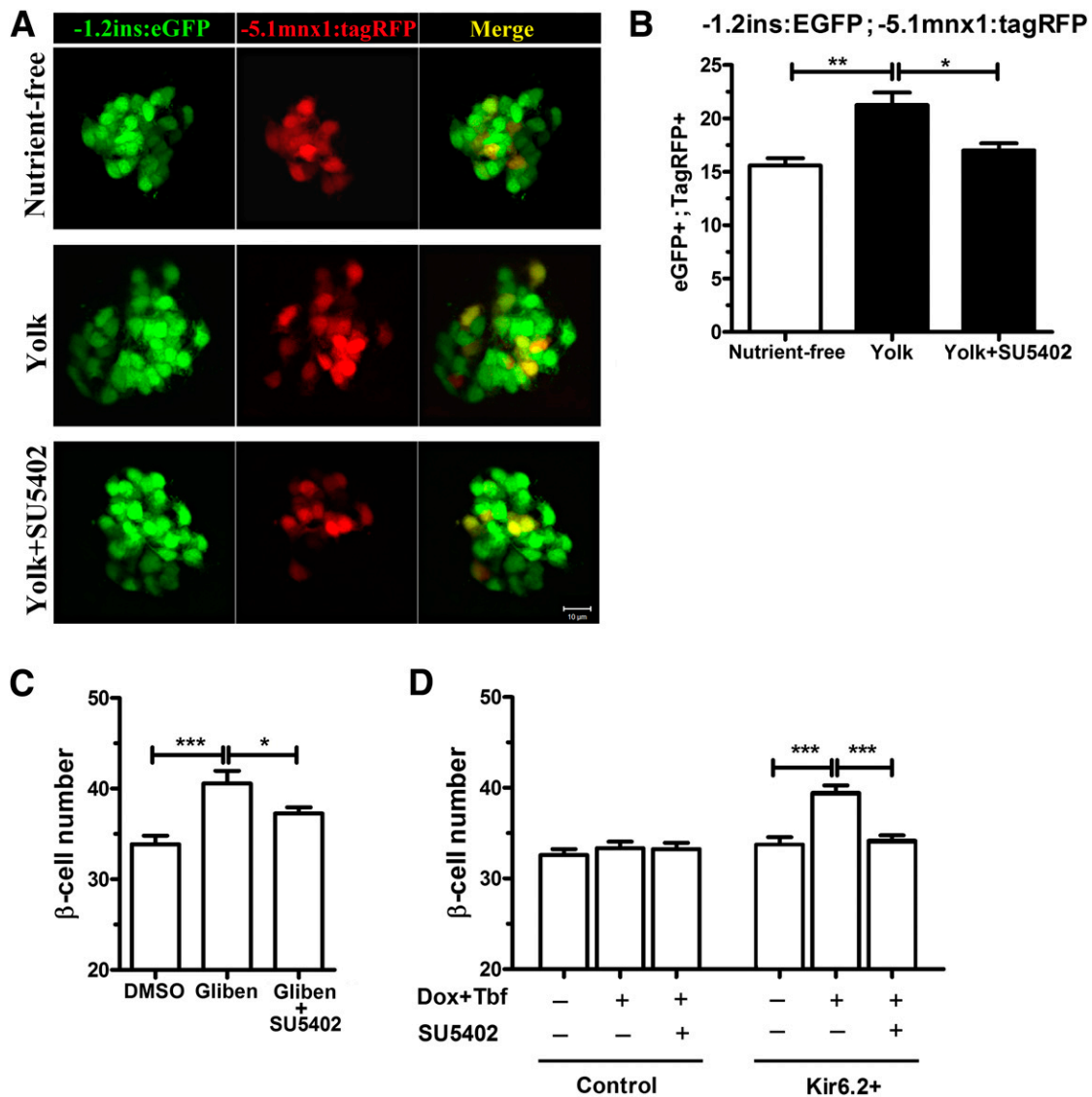


**Figure 2**—Inhibition of FGF signaling blocks overnutrition-induced differentiation. **A**: SU5402 inhibits yolk overnutrition-driven  $\beta$ -cell differentiation. Confocal projections of  $\beta$ -cells in 6-dpf  $Tg(-1.2ins:EGFP);Tg(-5.1mnx1:tagRFP)$  larvae after 8-h culture in nutrient-free medium, 5% egg yolk, or 5% egg yolk plus SU5402. Scale bar indicates 10  $\mu$ m. **B**: Quantification of tagRFP-positive  $\beta$ -cells in each group;  $n = 5$ –9. **C**: SU5402 inhibited glibenclamide (Gliben)-induced  $\beta$ -cell differentiation. 6-dpf  $Tg(-1.2ins:H2BmCherry)$  larvae were treated for 8 h with DMSO, glibenclamide, or glibenclamide plus SU5402.  $n = 11$ –16. **D**: SU5402 inhibition of  $\beta$ -cell differentiation induced by genetic suppression of  $K_{ATP}$  channel subunit, Kir6.2<sup>DN</sup>. Expression of a dominant-negative KIR6.2 (Kir6.2<sup>DN</sup>) in  $\beta$ -cells of 6-dpf  $Tg(-1.2ins:Kir6.2^{DN}-GFP^{TE-ON};LR)$  larvae is predicted to depolarize the plasma membrane and mimics overnutrition.  $Tg(-1.2ins:Kir6.2^{DN}-GFP^{TE-ON};LR);Tg(-1.2ins:H2BmCherry)$  larvae were treated with doxycycline (Dox) and tebufenozide (Tbf) to induce Kir6.2<sup>DN</sup>.  $n = 15$ –25. All data were analyzed by one-way ANOVA. \* $P < 0.05$ ; \*\* $P < 0.01$ ; \*\*\* $P < 0.001$ .

*fgf10b* were also detectable in zebrafish  $\beta$ -cells (Supplementary Fig. 5). Expression of *fgf1b*, *fgf4*, *fgf7*, and *fgf10a* was not observed.

To determine whether *Fgf1* is required for overnutrition-induced  $\beta$ -cell differentiation, we generated loss-of-function alleles of *fgf1* using TALEN-mediated mutagenesis (39). From the TALEN-mutagenized founders, we identified two independent germline mutations, one with a 5-bp deletion (*mu1*) and the other a 7-bp deletion (*mu2*); both mutations result in a reading-frame shift and premature stop codon (Supplementary Fig. 6B). *fgf1* mutant animals

were adult viable and fertile, consistent with the phenotype of *Fgf1* mutant mice (15). In the absence of overnutrition, no difference in  $\beta$ -cell number was observed in WT, heterozygotes (*fgf1*<sup>+/-</sup>), homozygous (*fgf1*<sup>mu1/mu1</sup>), or trans-heterozygous mutants (*fgf1*<sup>mu1/mu2</sup>) (Fig. 3C and D and Supplementary Fig. 6C). In stark contrast to sibling controls, when the *fgf1*<sup>-/-</sup> mutant animals were tested in the overnutrition assay, the number of  $\beta$ -cells did not increase (Fig. 3C and D and Supplementary Fig. 6C). These results demonstrate that *fgf1* is necessary for overnutrition-induced  $\beta$ -cell differentiation.

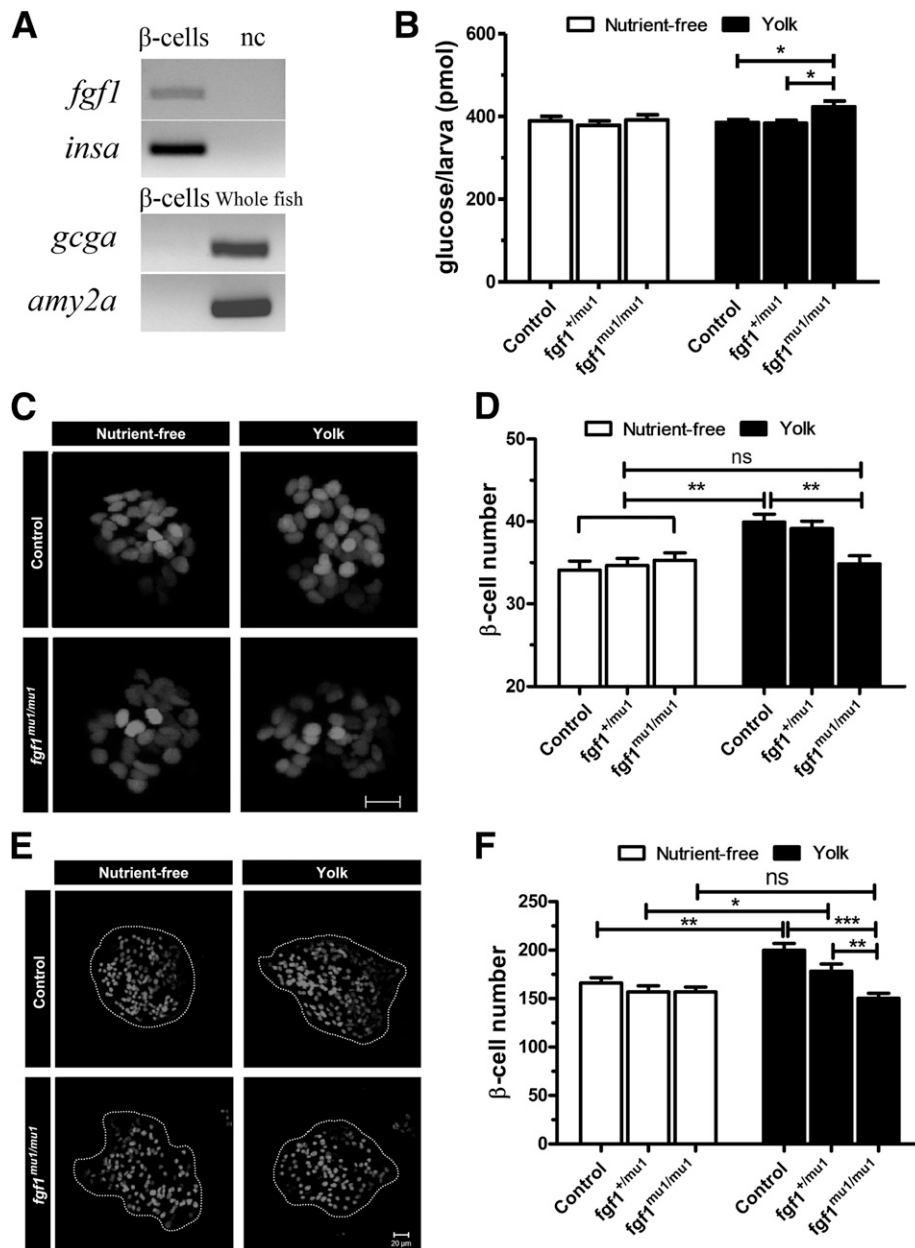


**Figure 3**—FGF1 is necessary for overnutrition-induced  $\beta$ -cell differentiation. **A**: RT-PCR analysis of *fgf1*, *insa*, *gcga*, and *amy2a* expression in FACS-sorted  $\beta$ -cells. nc, no template control. **B**: Overnutrition-induced mild hyperglycemia in *fgf1*<sup>mu1/mu1</sup> fish. Wild-type and *fgf1*<sup>mu1/mu1</sup> larvae were cultured for 8 h in nutrient-free or 5% egg yolk solution at 6 dpf, and their total free glucose levels were determined immediately after.  $n = 10$ . Representative confocal projections of  $\beta$ -cells of 6-dpf (**C**) and 4-week-old (**E**) *Tg(-1.2ins:H2B-mCherry)* or *fgf1*<sup>mu1/mu1</sup>; *Tg(-1.2ins:H2B-mCherry)* larvae cultured for 8 h in nutrient-free medium or 5% egg yolk. Scale bar indicates 10  $\mu$ m in **C** and 20  $\mu$ m in **E**. Quantification of  $\beta$ -cell number from 6-dpf larvae (**D**) or 4-week-old fish (**F**) suggested a loss of overnutrition-induced  $\beta$ -cell differentiation in *fgf1*-deficient fish.  $n = 7$ –24 in **D** and  $n = 10$  in **F**. \* $P < 0.05$ ; \*\* $P < 0.01$ ; \*\*\* $P < 0.001$ .

To assess the consequence of the failure of compensatory  $\beta$ -cell differentiation, we measured total glucose levels of these larvae at 6 dpf after overnutrition. In the absence of overnutrition, both *fgf1*<sup>-/-</sup> and wild-type larvae showed comparable levels of total glucose. However, with overnutrition, wild-type larvae maintained glucose levels that were not distinguishable from control animals, whereas *fgf1*<sup>-/-</sup> larvae had significantly elevated levels of total glucose (Fig. 3B). This result argues that the newly

formed  $\beta$ -cells are required for glucose homeostasis during overnutrition.

We were next interested in determining whether the Fgf1-mediated compensatory  $\beta$ -cell differentiation was a specific property of young larval zebrafish or whether this mechanism is functional in older animals. We tested the response of 4-week-old juvenile fish to 8 h of overnutrition with 5% chicken egg yolk.  $\beta$ -Cell number increased in response to overnutrition in WT, but not

*fgf1*<sup>-/-</sup> mutants (Fig. 3E and F). It is also interesting to note that the response in heterozygotes was also significantly abated (Fig. 3F). Of particular interest is the observation that  $\beta$ -cell number was not significantly decreased in the *fgf1*<sup>-/-</sup> mutants in the absence of overnutrition (Fig. 3E and F), strongly implying that *fgf1* is not required for normal  $\beta$ -cell proliferation, differentiation, or maintenance under normal husbandry conditions. Instead, *fgf1* appears to be critical only in response to overnutrition.

### Fgf1 Expressed Solely in $\beta$ -Cells Is Sufficient for Overnutrition-Induced $\beta$ -Cell Differentiation

From the preceding experiments it is clear that *fgf1* is required for overnutrition-induced  $\beta$ -cell differentiation. Previous work demonstrated that the  $\beta$ -cells act as the primary sensors that detect and signal the overnutrition state (24). We next asked whether *fgf1* expression solely in  $\beta$ -cells is sufficient to rescue the defective compensation in global *fgf1*<sup>-/-</sup> mutants. We expressed a human *FGF1* cDNA under the control of the zebrafish insulin promoter in  $\beta$ -cells in animals that were otherwise *fgf1*<sup>-/-</sup>. Thus, the only source for FGF1 in these animals was  $\beta$ -cells (Fig. 4A). In the WT background, the transgenic fish had a normal number of  $\beta$ -cells in normal conditions and responded to overnutrition like their wild-type siblings (Fig. 4B). In stark contrast to *fgf1*<sup>-/-</sup> animals that did not respond to overnutrition, *fgf1*<sup>-/-</sup> animals that expressed FGF1 in  $\beta$ -cells had a normal compensatory  $\beta$ -cell differentiation following overnutrition (Fig. 4C). Expression of FGF1 did not induce  $\beta$ -cell replication since no EdU incorporation was detected in  $\beta$ -cells (Supplementary Fig. 7), as observed previously (23). Thus, FGF1 expressed solely in  $\beta$ -cells is sufficient for overnutrition-induced  $\beta$ -cell differentiation. Critically, overexpression alone was not sufficient to drive  $\beta$ -cell differentiation in the absence of overnutrition, consistent with a model in which FGF1 activity is regulated posttranscriptionally, presumably through regulation of secretion.

If overnutrition induces  $\beta$ -cell differentiation by triggering *Fgf1* release from  $\beta$ -cells, then constitutive secretion of FGF1 from  $\beta$ -cells should induce  $\beta$ -cell differentiation in the absence of overnutrition. To bypass FGF1's nonclassical, signal peptide-independent secretion mechanism (18), we generated transgenic lines that express FGF1 fused to an N-terminal signal peptide, *Tg(-1.2ins:spFGF1)*. As expected, FGF1 was specifically expressed in  $\beta$ -cells in the transgenic lines (Fig. 4D). The engineered FGF1 is expected to be constitutively secreted through the canonical ER/Golgi secretory pathway (40). Fish that express the constitutively secreted spFGF1 had significantly more  $\beta$ -cells in the absence of overnutrition ( $39.3 \pm 1.3$  vs.  $34.2 \pm 0.9$ ) (Fig. 4E and Supplementary Fig. 8). Thus, constitutive secretion of FGF1 is sufficient to induce precocious differentiation of  $\beta$ -cells, even in the absence of overnutrition, strongly

implying that *Fgf1* secretion is the regulated step in mediating overnutrition-induced  $\beta$ -cell differentiation. Interestingly, overnutrition did not increase the  $\beta$ -cell number to more than control animals (Fig. 4E), suggesting the existence of a brake mechanism. These data demonstrate that FGF1 secreted from  $\beta$ -cells is sufficient to induce  $\beta$ -cell differentiation and that overnutrition likely triggers the release of FGF1 from  $\beta$ -cells.

### Mammalian INS-1 Cells Secrete FGF1 in Response to a Persistent Activation

Having demonstrated that *Fgf1* release from persistently activated  $\beta$ -cells due to overnutrition is sufficient to drive differentiation of  $\beta$ -cells in larval- and juvenile-stage zebrafish, we wished to determine whether this is unique to zebrafish or also occurs in mammalian cells. To determine whether mammalian  $\beta$ -cells respond to persistent activation with FGF1 release, a stable FGF1-expressing INS-1 832/13 cell line was generated. The INS-1 832/13-FGF1 cells expressed FGF1 at high levels (Supplementary Fig. 9). Activation of the insulin secretory apparatus of these cells with glibenclamide for 2 or 4 h did not result in increased FGF1 release. However 8 h of glibenclamide treatment increased FGF1 release in the conditioned medium (Fig. 5A and B). This is consistent with the results observed in zebrafish in which overnutrition or glibenclamide treatment must persist for >4 h to induce differentiation (23,24). Further, both of the Cu<sup>2+</sup> chelators neocuproine and U0126 blocked FGF1 release induced by glibenclamide (Fig. 5C and D), confirming our initial hypothesis.

### ER Stress Is a Signal of Overnutrition

Several lines of evidence have implicated ER stress in maintaining  $\beta$ -cell health during increased metabolic demand, including persistent glibenclamide treatment (41). To determine whether ER stress contributes to glibenclamide-induced  $\beta$ -cell differentiation, we tested whether pharmacologically relieving ER stress can reduce FGF1 release. As expected, the chemical chaperone TUDCA that has been shown to reduce ER stress in other systems (42) significantly reduced FGF1 release (Fig. 6A and B). Moreover, when INS-1 832/13-FGF1 cells were incubated with the ER stress inducer tunicamycin in the absence of glibenclamide, FGF1 release was increased (Fig. 6C and D). These results suggest that in mammalian  $\beta$ -cells, ER stress is sufficient to trigger FGF1 release and is necessary for persistent activation-induced FGF1 release.

To determine whether ER stress is also involved in overnutrition-induced  $\beta$ -cell differentiation in vivo, we performed an ultrastructural analysis of the  $\beta$ -cells in the islet of the 6-dpf zebrafish larvae with or without overnutrition. Interestingly, the  $\beta$ -cells in animals with overnutrition displayed mild ER stress. Specifically, the ER lumen of fish in overnutrition was dilated compared with unfed controls (Fig. 6E and F). To determine



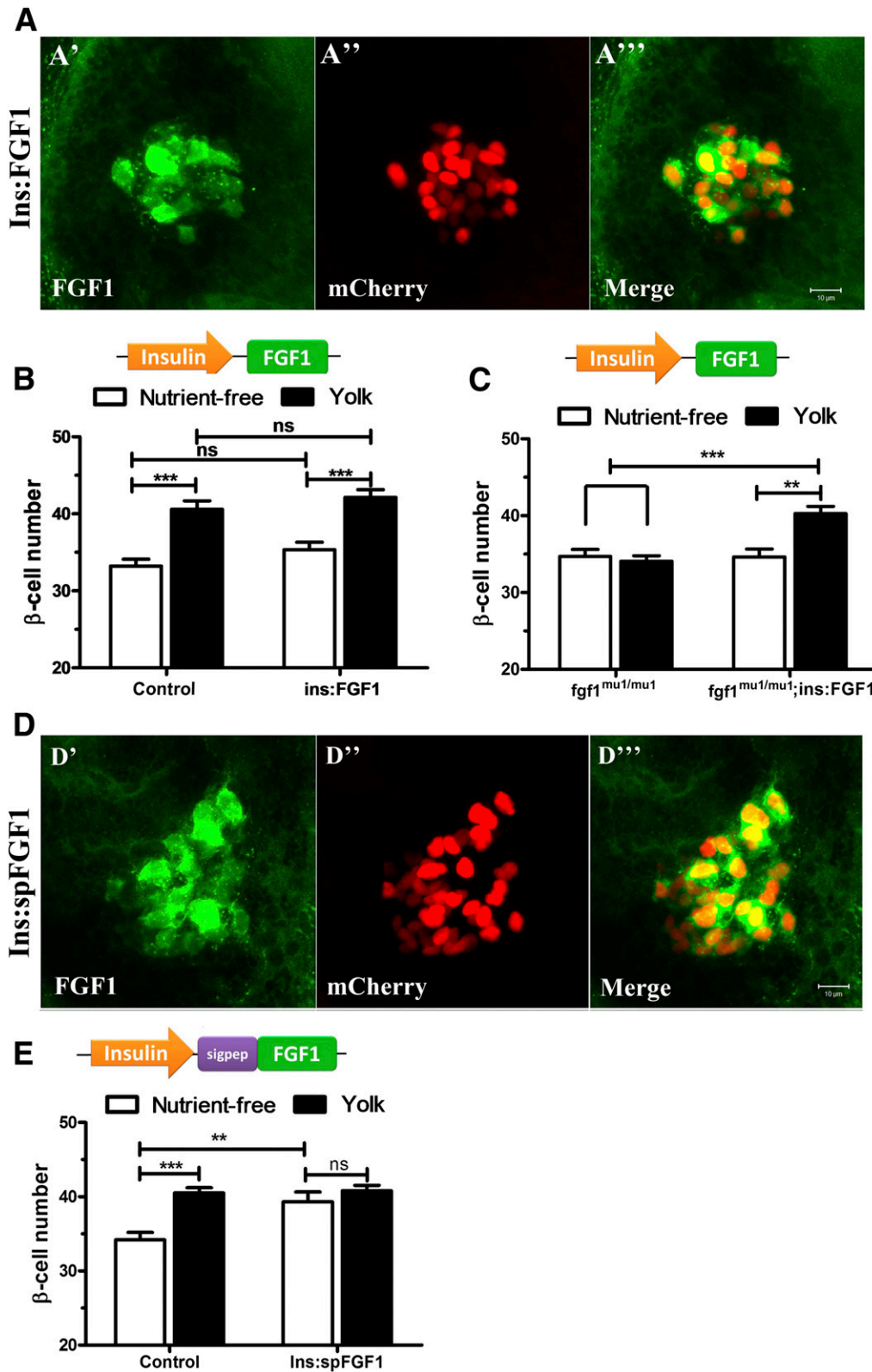


**Figure 4**—FGF1 is sufficient for overnutrition-induced  $\beta$ -cell differentiation. **A**: Confocal projections of FGF1 immunofluorescence in *fgf1*<sup>mu1/mu1</sup>;Tg(-1.2ins:FGF1; CG);Tg(-1.2ins:H2BmCherry) showing coexpression of FGF1 and mCherry. FGF1 was detected using an antibody specific for human FGF1 (A').  $\beta$ -Cells were marked by nuclear mCherry (A''). Scale bars indicate 10  $\mu$ m. **B**:  $\beta$ -Cell-specific expression of FGF1 does not alter  $\beta$ -cell number with or without overnutrition in wild-type fish. *n* = 10–12. **C**: Rescue of overnutrition-induced  $\beta$ -cell differentiation by  $\beta$ -cell-specific overexpression of human FGF1 in *fgf1*<sup>mu1/mu1</sup>, demonstrating that  $\beta$ -cell-specific expression is sufficient for overnutrition-induced  $\beta$ -cell differentiation; *n* = 12–18. **D**: Confocal projections of FGF1 immunofluorescence from Tg(-1.2ins:spFGF1; CG);Tg(-1.2ins:H2BmCherry) fish showing coexpression of FGF1 and mCherry. FGF1 was detected using an antibody

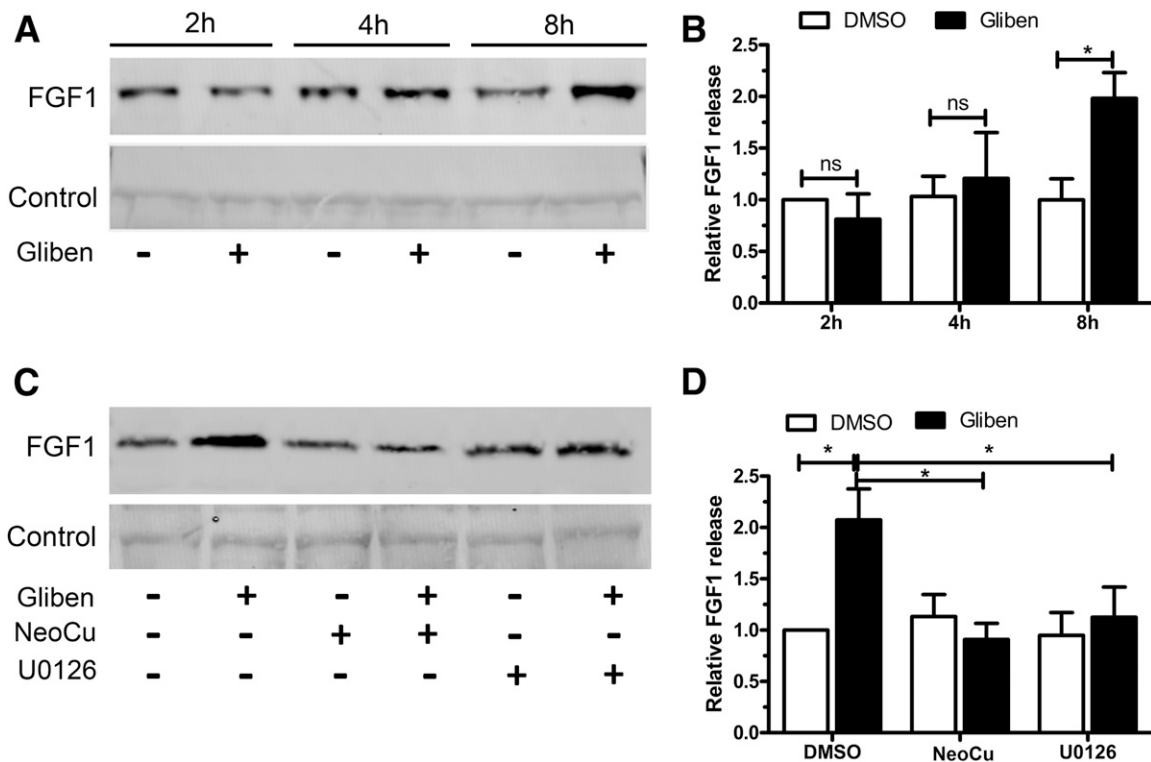


**Figure 5**—Prolonged activation of mammalian  $\beta$ -cells in vitro increases FGF1 release and FGF1 release requires copper. **A:** Representative Western blot of conditioned media from Ins-1 832/13-FGF1 cells incubated with 100 nmol/L glibenclamide (Gliben) for 2, 4, and 8 h. Upper panel is FGF1 and lower panel is a nonspecific band serving as an internal control. DMSO (0.1%) was used as a vehicle control (–). **B:** Quantification of the relative FGF1 release from lengths of treatment. The level of FGF1 normalized to the nonspecific band was set to 1 for the control sample at the 2-h time point. The graphs represent three independent biological repeats. FGF1 in the media was significantly increased after 8 h of treatment. **C:** Representative Western blot of Ins-1 832/13-FGF1 cells incubated with 100 nmol/L Gliben or Gliben plus copper chelators (neocuproine, NeoCu, and U0126) for 8 h. DMSO (0.1%) was used as the vehicle control. **D:** Quantification of the relative FGF1 release from glibenclamide in the presence of copper chelators. The level of FGF1 normalized to the nonspecific band was set to 1 for the DMSO-only group. The graph represents four biological repeats. All data were analyzed by one-way ANOVA. \* $P < 0.05$ .

whether ER stress contributes to the generation of the overnutrition-induced  $\beta$ -cell differentiation, we performed the overnutrition-induced  $\beta$ -cell differentiation assay in the presence or absence of TUDCA. TUDCA blocked compensatory  $\beta$ -cell differentiation (Fig. 6G), suggesting that ER stress is required for the compensatory  $\beta$ -cell differentiation. These results argue that  $\beta$ -cell ER stress contributes to overnutrition-induced  $\beta$ -cell differentiation by triggering the release of Fgf1 from  $\beta$ -cells.

## DISCUSSION

Under conditions of heightened insulin demand, for example overnutrition or insulin resistance,  $\beta$ -cell mass increases to meet the heightened insulin demand. In contrast to normal  $\beta$ -cell development, relatively little is known about the mechanisms of compensatory  $\beta$ -cell

differentiation. We have developed a system that allows us to probe the molecular mechanisms by which increased insulin demand during acute overnutrition results in a rapid, compensatory increase in  $\beta$ -cell number (23,24). Applying a combination of pharmacological and genetic manipulations in the zebrafish model of compensatory  $\beta$ -cell differentiation, we demonstrate a novel physiological function of Fgf1 in  $\beta$ -cell mass homeostasis in response to overnutrition.

Four FGF ligands have been studied in the context of pancreas development in zebrafish (43–46). These studies show that *fgf3* and *fgf8* are required for  $\beta$ -cell differentiation (46), *fgf10* is required to prevent ectopic  $\beta$ -cell differentiation (41), and *fgf24* is required for ventral pancreatic bud formation (43). We now ascribe a novel physiological function to Fgf1 in  $\beta$ -cell dynamics. Unlike the previously studied FGFR ligands, *fgf1*<sup>−/−</sup> zebrafish

specific for human FGF1 (*D'*).  $\beta$ -Cells were marked by nuclear mCherry (*D''*). Scale bars indicate 10  $\mu$ m. **E:**  $\beta$ -Cell-specific overexpression of a constitutively secreted FGF1 results in an increase in  $\beta$ -cell number in nutrient-free conditions compared with that seen in the overnutrition state, indicating that secretion from  $\beta$ -cells induces  $\beta$ -cell differentiation. sigpep, signal peptide.  $n = 20$ –25. All data were analyzed by one-way ANOVA. \*\* $P < 0.01$ ; \*\*\* $P < 0.001$ .

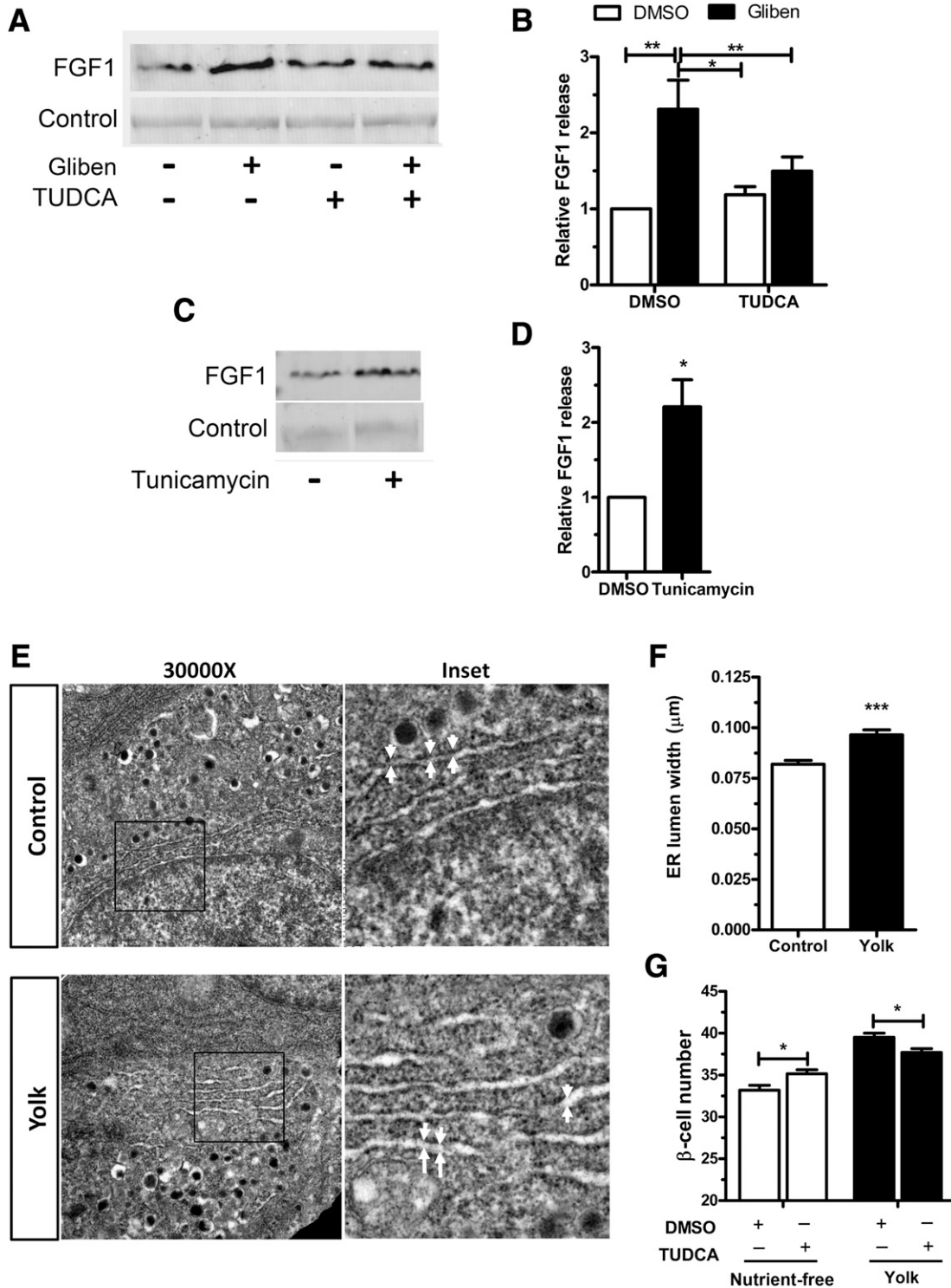


**Figure 6**—Overnutrition induces mild  $\beta$ -cell ER stress. **A**: Representative Western blot of Ins-1 832/13-FGF1 cells incubated with DMSO, 100 nmol/L glibenclamide (Gliben), or glibenclamide plus TUDCA for 8 h. DMSO (0.1%) was used as the vehicle control. **B**: Quantification of the relative FGF1 release from glibenclamide and TUDCA treatments. The level of FGF1 normalized to the nonspecific band was set to 1 for the DMSO-only group. The graph represents four biological repeats. **C**: Representative Western blot of Ins-1 832/13-FGF1 cells incubated with DMSO or tunicamycin for 8 h. **D**: Quantification of the relative FGF1 release with tunicamycin treatment compared with the DMSO-only treatments. Graphs represent four independent biological repeats. **E**: Electron micrographs of  $\beta$ -cells from unfed fish and egg yolk-fed fish. Yolk-fed fish show mild ER dilation compared with unfed controls. White arrows show the ER in the cells. **F**: The width of the ER lumen was measured in the rough ER for five cells in each group at 20 or more positions per cell. Statistical analysis of ER lumen dilation in unfed fish and egg yolk-fed fish. **G**: Quantification of the  $\beta$ -cell number in 6-dpf *Tg(-1.2ins:H2BmCherry)* animals cultured in nutrient-free or 5% egg yolk solution containing DMSO or TUDCA for 8 h.  $n = 37$ –45. All data were analyzed by one-way ANOVA. \* $P < 0.05$ ; \*\* $P < 0.01$ ; \*\*\* $P < 0.001$ .

appear normal, healthy, and fertile, similar to *FGF1* mutant mice (15). They have normal  $\beta$ -cell numbers through larval and juvenile development under standard feeding and housing conditions, indicating that *fgf1* is not required for  $\beta$ -cell development. We show that *fgf1*<sup>-/-</sup> fish fail to respond to overnutrition with compensatory  $\beta$ -cell differentiation (Fig. 3C–F). Thus our studies add a novel physiological function to FGF1, in addition to the recently discovered metabolic function in mice (17),

Mechanistically, we propose that 8 h of overnutrition results in insulin demand that surpasses the insulin synthetic capacity of the existing  $\beta$ -cells; the resulting ER stress from attempting to meet this insulin demand triggers the release of FGF1. FGF1 then recruits new  $\beta$ -cells to differentiate. Our conclusion that FGF1 is necessary for  $\beta$ -cell differentiation following overnutrition comes from the result that *fgf1* mutants cannot respond to overnutrition by increasing  $\beta$ -cell number. In support of this result, overnutrition increases expression of FGF target genes, which is blocked by the FGFR antagonist SU5402. We were able to identify the cells that are critical for *Fgf1* release as  $\beta$ -cell-specific expression of FGF1 rescues the *fgf1* mutants (Fig. 4C). Expression of FGF1 in  $\beta$ -cells is sufficient to restore wild-type overnutrition response to *fgf1*<sup>-/-</sup> mutant animals. Moreover, we were able to demonstrate that *Fgf1* release is the key regulatory step as overexpression of FGF1 in  $\beta$ -cells alone is not sufficient to increase  $\beta$ -cell number, but overexpression of a constitutively secreted FGF1 in  $\beta$ -cells is sufficient to increase  $\beta$ -cell number even in the absence of overnutrition (Fig. 4E).

The results in INS-1 832/13 cells directly confirm that persistent activation leads to FGF1 secretion. Importantly, the in vitro model allows the discovery of a possible role of ER stress in FGF1 secretion during persistent activation, which we were then able to confirm in zebrafish (Fig. 6). Future vigorous experiments are necessary to more firmly establish the connection between ER stress and FGF1 release.

By studying the acute compensatory  $\beta$ -cell response to overnutrition in young larvae, we identified FGF1 as a necessary and sufficient signal that increases  $\beta$ -cell differentiation in response to overnutrition. The advantage of studying an acute system that responds rapidly is the ability to investigate the compensatory pathway in a system of reduced complexity. The mechanism also occurs in larval zebrafish and in juvenile zebrafish (Fig. 3E and F). We do not know if similar mechanisms exist for compensatory  $\beta$ -cell mass regulation in mammals since no equivalent model has been developed. However, it is likely that ER stress-dependent FGF1 release in  $\beta$ -cells does occur in mammals in vivo. As  $\beta$ -cell ER stress is a common consequence of increased metabolic load (47), it is not unreasonable to expect enhanced FGF1 signaling in the peri-islet region in conditions of heightened insulin demand in mammals. The response to this enhanced signaling may vary with species and age, however. If peri-islet FGF1 is found to increase  $\beta$ -cell mass, it may partially account for the recently reported antidiabetic function of recombinant FGF1 (17).

In closing, we propose that overnutrition can increase insulin demand beyond the synthetic capacity of existing

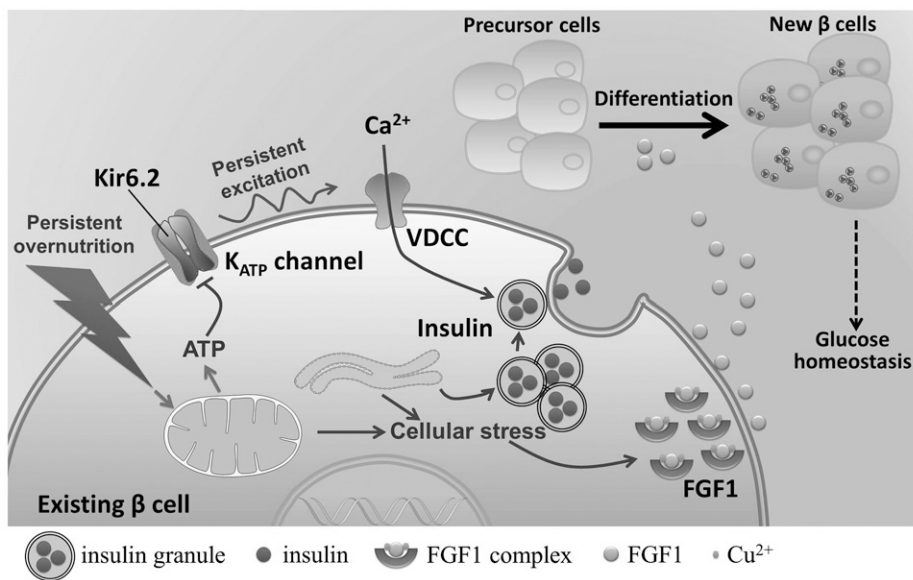


**Figure 7**—A working model for FGF1-mediated overnutrition-induced  $\beta$ -cell differentiation. Persistent overnutrition increases nutrient metabolism in  $\beta$ -cells and prolonged depolarization of the plasma membrane through closure of  $K_{ATP}$  channels. The subsequent prolonged release of insulin leads to enhanced protein synthesis and proinsulin processing in the ER to replenish insulin granules. This enhanced insulin synthesis may cause cellular stress. We propose that this cellular stress in  $\beta$ -cells leads to FGF1 release, which acts in a paracrine fashion to induce postmitotic endocrine precursor cells to differentiate into  $\beta$ -cells. This increase in  $\beta$ -cells increases insulin synthetic capacity, maintaining glucose homeostasis and reducing stress in the  $\beta$ -cell population, restoring homeostasis.

$\beta$ -cells; this would be expected to generate stress in  $\beta$ -cells. The cellular stress likely triggers *Fgf1* release, which in turn drives differentiation of an undifferentiated cell population into  $\beta$ -cells. This increases  $\beta$ -cell mass and the net insulin synthetic capacity. The increase in  $\beta$ -cell mass in turn restores glucose homeostasis (Fig. 7).

**Acknowledgments.** The authors thank Lisette A. Maddison (Vanderbilt University) for constructive discussions and critical reading of the manuscript. The authors thank Shu-Yu Wu (Vanderbilt University) for providing the *erm* and *spry4* probes. The authors appreciate the expert technical support from Vanderbilt Flow Cytometry Shared Resource for cell sorting, and from Amanda Goodrich and Corey Guthrie in the Vanderbilt Zebrafish Core Facility for excellent care of the zebrafish.

**Funding.** This work was supported by the Vanderbilt Diabetes Research and Training Center and DK-088686 (W.C.), and by American Diabetes Association grant 1-13-BS-027 (W.C.). The authors utilized the core(s) of the Vanderbilt Diabetes Research and Training Center funded by grant DK-02593 from the National Institute of Diabetes and Digestive and Kidney Diseases, and confocal imaging was performed in the VUMC Cell Imaging Shared Resource (supported by National Institutes of Health grants CA68485, DK20593, DK58404, HD15052, DK59637, and EY08126).

**Duality of Interest.** No potential conflicts of interest relevant to this article were reported.

**Author Contributions.** M.L. conceived and designed the research; performed experiments; analyzed data; interpreted results of experiments; prepared figures; and drafted, edited, revised, and approved the final version of the manuscript. P.P.-M. analyzed data, interpreted results of experiments, and edited and revised the manuscript. W.C. conceived and designed the research; performed experiments; analyzed data; interpreted results of experiments; and edited, revised, and approved the final version of the manuscript. W.C. is the guarantor of this work and, as such, had full access to all the data in the study and takes responsibility for the integrity of the data and the accuracy of the data analysis.

## References

- Lysy PA, Weir GC, Bonner-Weir S. Concise review: pancreas regeneration: recent advances and perspectives. *Stem Cells Transl Med* 2012;1:150–159
- Yeohor V, Chan L. Minireview: beta-cell replacement therapy for diabetes in the 21st century: manipulation of cell fate by directed differentiation. *Mol Endocrinol* 2010;24:1501–1511
- Prentki M, Nolan CJ. Islet beta cell failure in type 2 diabetes. *J Clin Invest* 2006;116:1802–1812
- Flier SN, Kulkarni RN, Kahn CR. Evidence for a circulating islet cell growth factor in insulin-resistant states. *Proc Natl Acad Sci U S A* 2001;98:7475–7480
- El Ouaamari A, Kawamori D, Dirice E, et al. Liver-derived systemic factors drive  $\beta$  cell hyperplasia in insulin-resistant states. *Cell Reports* 2013;3:401–410
- Bouwens L, Rooman I. Regulation of pancreatic beta-cell mass. *Physiol Rev* 2005;85:1255–1270
- Bernal-Mizrachi E, Kulkarni RN, Scott DK, Mauvais-Jarvis F, Stewart AF, Garcia-Ocaña A. Human  $\beta$ -cell proliferation and intracellular signaling part 2: still driving in the dark without a road map. *Diabetes* 2014;63:819–831
- Kulkarni RN, Mizrachi EB, Ocana AG, Stewart AF. Human  $\beta$ -cell proliferation and intracellular signaling: driving in the dark without a road map. *Diabetes* 2012;61:2205–2213
- Okada T, Liew CW, Hu J, et al. Insulin receptors in beta-cells are critical for islet compensatory growth response to insulin resistance. *Proc Natl Acad Sci U S A* 2007;104:8977–8982
- Gu D, Sarvetnick N. Epithelial cell proliferation and islet neogenesis in IFN- $\gamma$  transgenic mice. *Development* 1993;118:33–46
- Wang TC, Bonner-Weir S, Oates PS, et al. Pancreatic gastrin stimulates islet differentiation of transforming growth factor alpha-induced ductular precursor cells. *J Clin Invest* 1993;92:1349–1356
- Friesel R, Maciag T. Fibroblast growth factor prototype release and fibroblast growth factor receptor signaling. *Thromb Haemost* 1999;82:748–754
- Zakrzewska M, Marcinkowska E, Wiedlocha A. FGF-1: from biology through engineering to potential medical applications. *Crit Rev Clin Lab Sci* 2008;45:91–135
- Raju R, Palapetta SM, Sandhya VK, et al. A Network Map of FGF-1/FGFR Signaling System. *J Signal Transduct*. 16 April 2014 [Epub ahead of print]. DOI: 10.1155/2014/962962
- Miller DL, Ortega S, Bashayan O, Basch R, Basilico C. Compensation by fibroblast growth factor 1 (FGF1) does not account for the mild phenotypic defects observed in FGF2 null mice. *Mol Cell Biol* 2000;20:2260–2268
- Jonker JW, Suh JM, Atkins AR, et al. A PPAR $\gamma$ -FGF1 axis is required for adaptive adipose remodelling and metabolic homeostasis. *Nature* 2012;485:391–394
- Suh JM, Jonker JW, Ahmadian M, et al. Endocrinization of FGF1 produces a neomorphic and potent insulin sensitizer. *Nature* 2014;513:436–439
- Prudovsky I, Mandinova A, Soldi R, et al. The non-classical export routes: FGF1 and IL-1 $\alpha$  point the way. *J Cell Sci* 2003;116:4871–4881
- Jackson A, Friedman S, Zhan X, Engleka KA, Forough R, Maciag T. Heat shock induces the release of fibroblast growth factor 1 from NIH 3T3 cells. *Proc Natl Acad Sci U S A* 1992;89:10691–10695
- Mouta Carreira C, Landriscina M, Bellum S, Prudovsky I, Maciag T. The comparative release of FGF1 by hypoxia and temperature stress. *Growth Factors* 2001;18:277–285
- Shin JT, Opalenik SR, Wehby JN, et al. Serum-starvation induces the extracellular appearance of FGF-1. *Biochim Biophys Acta* 1996;1312:27–38
- Ananyeva NM, Tjurmin AV, Berliner JA, et al. Oxidized LDL mediates the release of fibroblast growth factor-1. *Arterioscler Thromb Vasc Biol* 1997;17:445–453
- Maddison LA, Chen W. Nutrient excess stimulates  $\beta$ -cell neogenesis in zebrafish. *Diabetes* 2012;61:2517–2524
- Li M, Maddison LA, Page-McCaw P, Chen W. Overnutrition induces  $\beta$ -cell differentiation through prolonged activation of  $\beta$ -cells in zebrafish larvae. *Am J Physiol Endocrinol Metab* 2014;306:E799–E807
- Kimmel CB, Ballard WW, Kimmel SR, Ullmann B, Schilling TF. Stages of embryonic development of the zebrafish. *Dev Dyn* 1995;203:253–310
- Li M, Maddison LA, Crees Z, Chen W. Targeted overexpression of CKI-insensitive cyclin-dependent kinase 4 increases functional  $\beta$ -cell number through enhanced self-replication in zebrafish. *Zebrafish* 2013;10:170–176
- Suster ML, Kikuta H, Urasaki A, Asakawa K, Kawakami K. Transgenesis in zebrafish with the tol2 transposon system. *Methods Mol Biol* 2009;561:41–63
- Kwan KM, Fujimoto E, Grabher C, et al. The Tol2kit: a multisite gateway-based construction kit for Tol2 transposon transgenesis constructs. *Dev Dyn* 2007;236:3088–3099
- Cermak T, Doyle EL, Christian M, et al. Efficient design and assembly of custom TALEN and other TAL effector-based constructs for DNA targeting. *Nucleic Acids Res* 2011;39:e82
- Wang Y, Rovira M, Yusuff S, Parsons MJ. Genetic inducible fate mapping in larval zebrafish reveals origins of adult insulin-producing  $\beta$ -cells. *Development* 2011;138:609–617
- Delaspre F, Beer RL, Rovira M, et al. Centroacinar cells are progenitors that contribute to endocrine pancreas regeneration. *Diabetes* 2015;64:3499–3509
- Hesselton D, Anderson RM, Beinat M, Stainier DY. Distinct populations of quiescent and proliferative pancreatic beta-cells identified by H $\beta$ Cre mediated labeling. *Proc Natl Acad Sci U S A* 2009;106:14896–14901
- Ye L, Robertson MA, Hesselton D, Stainier DY, Anderson RM. Glucagon is essential for alpha cell transdifferentiation and beta cell neogenesis. *Development* 2015;142:1407–1417
- Hohmeier HE, Mulder H, Chen G, Henkel-Rieger R, Prentki M, Newgard CB. Isolation of INS-1-derived cell lines with robust ATP-sensitive K $^{+}$  channel-dependent

- and -independent glucose-stimulated insulin secretion. *Diabetes* 2000;49:424–430
35. Sun L, Tran N, Liang C, et al. Design, synthesis, and evaluations of substituted 3-[(3- or 4-carboxyethylpyrrol-2-yl)methylidene]indolin-2-ones as inhibitors of VEGF, FGF, and PDGF receptor tyrosine kinases. *J Med Chem* 1999;42:5120–5130
36. Ishizaki H, Spitzer M, Wildenhain J, et al. Combined zebrafish-yeast chemical-genetic screens reveal gene-copper-nutrition interactions that modulate melanocyte pigmentation. *Dis Model Mech* 2010;3:639–651
37. Madsen EC, Gitlin JD. Zebrafish mutants calamity and catastrophe define critical pathways of gene-nutrient interactions in developmental copper metabolism. *PLoS Genet* 2008;4:e1000261
38. Scholpp S, Brand M. Endocytosis controls spreading and effective signaling range of Fgf8 protein. *Curr Biol* 2004;14:1834–1841
39. Bedell VM, Wang Y, Campbell JM, et al. In vivo genome editing using a high-efficiency TALEN system. *Nature* 2012;491:114–118
40. Robinson ML, Overbeek PA, Verran DJ, et al. Extracellular FGF-1 acts as a lens differentiation factor in transgenic mice. *Development* 1995;121:505–514
41. Kim JY, Lim DM, Park HS, et al. Exendin-4 protects against sulfonylurea-induced  $\beta$ -cell apoptosis. *J Pharmacol Sci* 2012;118:65–74
42. de Almeida SF, Picarote G, Fleming JV, Carmo-Fonseca M, Azevedo JE, de Sousa M. Chemical chaperones reduce endoplasmic reticulum stress and prevent mutant HFE aggregate formation. *J Biol Chem* 2007;282:27905–27912
43. Dong PD, Munson CA, Norton W, et al. Fgf10 regulates hepatopancreatic ductal system patterning and differentiation. *Nat Genet* 2007;39:397–402
44. Manfroid I, Delporte F, Baudhuin A, et al. Reciprocal endoderm-mesoderm interactions mediated by fgf24 and fgf10 govern pancreas development. *Development* 2007;134:4011–4021
45. Naye F, Voz ML, Detry N, Hammerschmidt M, Peers B, Manfroid I. Essential roles of zebrafish bmp2a, fgf10, and fgf24 in the specification of the ventral pancreas. *Mol Biol Cell* 2012;23:945–954
46. Song J, Kim HJ, Gong Z, Liu NA, Lin S. Vhnf1 acts downstream of Bmp, Fgf, and RA signals to regulate endocrine beta cell development in zebrafish. *Dev Biol* 2007;303:561–575
47. Papa FR. Endoplasmic reticulum stress, pancreatic  $\beta$ -cell degeneration, and diabetes. *Cold Spring Harb Perspect Med* 2012;2:a007666